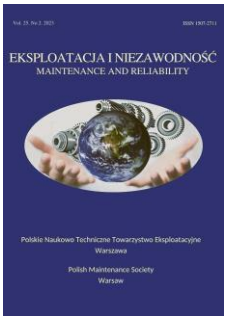

Eksploatacja i Niezawodnosc – Maintenance and Reliability
Volume 28 (2026), Issue 4
journal homepage: http://www.ein.org.pl

Article citation info:
Lin S, Liu C, Jia L, Zhang H, Zhang P, Yu B, Decision-oriented reliability assessment of complex mechatronic systems based on stochastic flow networks, Eksploatacja i Niezawodnosc – Maintenance and Reliability 2026: 28(4) http://doi.org/10.17531/ein/220118

Decision-oriented reliability assessment of complex mechatronic systems based on stochastic flow networks

Indexed by: Web of Science Group

Shuai Lin[a], Cuifang Liu[a], Limin Jia[b], Hengrun Zhang[c,*], Pengzhu Zhang[d], Benhai Yu[a]

[a] Shanghai Institute of Technology, China
[b] Beijing Jiaotong University, China
[c] East China University of Science and Technology, China
[d] Shanghai Jiao Tong University, China

Highlights

- The MSFN framework is developed to describe system topology and functions.
- Layer reliability and local reliability are introduced to analysis system reliability.
- Cognitive uncertainty for experts is mitigated using an integrated fuzzy-MTS approach.
- A trade-off between decision timeliness and assessment accuracy is quantified.

Abstract

Conventional reliability assessments for complex mechatronic systems (CMS) often fail to fully account for the specific demands of operational management and maintenance decision-making. To bridge this gap, a hierarchical system reliability modeling approach that combines stochastic flow networks with fuzzy logic theory is introduced. Specifically, a multi-layer stochastic flow network (MSFN) is constructed to simultaneously capture the holistic topology and its dynamic functional execution mechanisms. In this model, minimal paths (MPs) are employed to calculate layer reliability under flow constraints. Concurrently, the 2-additive Choquet integral functions as an aggregation operator to quantify dependencies between different layers. Furthermore, to reduce cognitive uncertainty in expert elicitation, interval hesitant fuzzy sets are combined with the Mahalanobis-Taguchi System. Finally, a functional operator is constructed for system reliability assessment across different decision-making scenarios. Application to an urban rail train system confirms the effectiveness of the proposed method in providing targeted decision support across diverse management departments.

Keywords
system reliability, complex mechatronic systems, stochastic flow networks, fuzzy theory, management decision-making

1. Introduction

Complex mechatronic systems (CMSs) are typically characterized by intricate structures, multi-functionality, high performance, heavy loads, and variable operating environments [1]. Consequently, compared to conventional systems, they exhibit a higher failure probability and more complex failure modes, making them more susceptible to major catastrophic accidents [2]. In practical engineering applications, various management decisions rely heavily on the results of system reliability assessments [3,4]. However, existing research often overlooks the specific requirements of different decision-making scenarios, leading to significant assessment errors and low efficiency, which can ultimately compromise the effectiveness of management decisions. Therefore, there is an urgent need to conduct system reliability analysis for CMSs tailored to diverse management decision requirements, providing a critical reference for ensuring the robust and safe

(*) Corresponding author.
E-mail addresses: S. Lin (ORCID: 0000-0001-8180-4905) linshuai2013@126.com, C. Liu (ORCID: 0009-0004-8135-2303) 1206575004@qq.com, L. Jia (ORCID: 0000-0001-9949-4861) bjlwtg2013@163.com, H. Zhang (ORCID: 0000-0002-7405-9588) zhanghengrun@ecust.edu.cn, P. Zhang (ORCID: 0009-0004-4976-6768) pzztgao2020@yeah.net, B. Yu (ORCID: 0009-0009-3412-1365) ybh@sit.edu.cn

operation of these systems.

Currently, few studies on the reliability of CMSs account for the specific requirements of diverse management decisions, such as timeliness and computational accuracy. Existing studies mainly consider the impact of system functions, holistic topology, and related data on system reliability. Early methods based on traditional reliability theory were predominant and widely applied to the reliability analysis of critical subsystems within CMSs [5,6]. These methods modeled the functional structure of CMSs and evaluated their reliability by integrating relevant failure data into models based on fault tree analysis [7], Petri nets [8], Bayesian networks [9], Markov processes [10], dynamic fault trees [6] and the Go methodology [11]. However, drawbacks such as state space explosion, modeling difficulties, and unrealistic assumptions have limited their applicability to system-level reliability studies.

With the advancement of deep learning technologies, data-driven reliability analysis methods have emerged [12,13]. By leveraging full-lifecycle monitoring data, these methods establish the implicit mapping between data features and the system's health status using statistical or machine learning algorithms, such as neural networks [14], Long Short-Term Memory (LSTM) networks [15] and Monte Carlo simulation [16]. Consequently, system reliability can be estimated without the need for a thorough understanding of the complex internal mechanisms. Nevertheless, these methods often suffer from opaque relationships between component performance and system reliability, poor interpretability, high computational complexity, and significant resource consumption, which hinder their practical application in engineering.

In recent years, to overcome the limitations of the aforementioned approaches, some scholars have begun to integrate network theory into the reliability research of CMSs [17–19]. By abstracting the holistic topology of the system into a network model and constructing network reliability measures based on functional attributes, the results of the network reliability are analyzed to represent the system reliability, such as centrality reliability [20], connectivity coefficient [21], percolation reliability [22], network reliability [23]. This approach not only achieves holistic topological modeling but also clarifies the relationship between component performance and system reliability while incorporating relevant data parameters.

Research grounded in network theory involves two core aspects:

1) Networking of CMSs. Given that system reliability is intrinsically linked to functions, and topology determines functions, modeling the holistic structure is the fundamental basis for system reliability assessment [24]. Consequently, the fidelity of the constructed network model directly dictates the accuracy and precision of the system reliability evaluation. Existing studies typically treat components or minimum maintenance units (MMUs) as nodes and their physical connections as edges, abstracting the topology of CMSs into a single-layer directed network. For instance, Liu et al. [25] represented an aircraft engine system as a network where nodes denote components and directed edges represent physical coupling. Lin S et al. [19] noted the difficulty in obtaining parameter data for certain components and thus proposed a high-speed train system topological network where nodes and edges represent MMUs and their connection relationships, respectively. Xia et al. [26] considered the heterogeneity of connections and constructed a mechanical-electrical-control three-layer network model, using edge types as the basis for stratification. Although recent research has begun to address the heterogeneity of connections, the specific impact of different connections on performance has yet to be incorporated into system reliability assessment. In addition, the aforementioned networks fail to capture the dynamic process of function execution.

2) Construction of network reliability measures. Network reliability measures provide the basis for evaluating system reliability and reflect the relationship between node performance and system reliability. For instance, Wang et al. [23] constructed the task reliability of Gas-Insulated Metal-Enclosed Transmission Line (GIL) equipment systems based on failure propagation probability and Copula function. Yin et al. [20] treated the strength of connection relationships between nodes as edge weights and presented a system reliability index considering community structure and clustering coefficients. Lin S et al. [19] incorporated percolation theory to propose percolation reliability based on betweenness, degree, and node reliability. Liu et al. [27] introduced node propagation coefficients and node centrality to define network effectiveness

for system reliability analysis. Essentially, these measures enhance network reliability metrics by integrating node attributes. However, due to the neglect of the realization process of dynamic system functions, these methods remain essentially an analysis of structural reliability. Therefore, some researchers argue that such studies are applicable only to structural analysis during the design phase and are not suitable for management decisions in the operation and maintenance phase.

In recent years, research on the reliability of stochastic flow networks (SFNs) has yielded significant achievements and has been applied to the reliability assessment of complex networked systems [28], such as transportation systems [29], grid power systems [30], supply chain systems [31], manufacturing network systems [32], and sensor networks [33]. An SFN typically refers to a stochastic network in which both the whole network and its constituent units possess multiple distinct performance levels; that is, beyond basic connectivity requirements, a certain amount of flow must be transmitted to ensure the network maintains a specific throughput [34]. Compared to traditional networks, SFNs provide a more comprehensive description of the holistic topology and dynamic function implementation of CMSs. Specifically, the connection relationships between nodes and edges represent the inherent topological structure of the system, the flow transmission process describes the execution of dynamic system functions, and the throughput reflects the system's parameter data. Furthermore, the capacity or the product flow handled by the connections (edges) between various components in a CMS is not fixed, but rather multi-state and stochastic. Consequently, it is more reasonable to model the CMS as an SFN.

Therefore, based on the SFNs and fuzzy theory, this paper proposes a system reliability assessment method for CMSs adaptable to diverse management decision-making scenarios. The main contributions of this paper are summarized as follows:

(1) The CMS is abstracted as a multi-layer stochastic flow network (MSFN), where nodes and edges represent topological properties, and attribute sets denote functional features.

(2) Layer reliability and local reliability are introduced, and then the algorithm based on minimal paths (MPs) for the layer reliability evaluation and the local reliability model based on the 2-additive Choquet integral are presented, respectively.

(3) A system reliability model is proposed that aggregates local reliabilities via functional operators to accommodate diverse management decisions.

The rest of this paper is organized as follows. Section 2 reviews the basics and preliminaries. In Section 3, the construction method of the MSFN for the CMS is proposed. In Section 4, the system reliability model for different management decisions is developed based on layer reliability, local reliability and functional operators. Section 5 illustrates the examples as well as benchmarks. Finally, the conclusion and future work are presented in Section 6.

2. Basics and preliminaries

2.1. Stochastic flow networks

Let $G \equiv (V, E, M)$ denote a stochastic flow network (SFN) with a source s and sink t. Then, we have a node set $V = \{v_i | 1 \le i \le n\}$, an edge set $E = \{e_{ij} | i \ne j \; for \; 1 \le i \le n-1, 2 \le j \le n\}$, and a maximal capacity set $M = \{m_{ij} | i \ne j \; for \; 1 \le i \le n-1, 2 \le j \le n\}$. m_{ij} is the maximal capacity of the edge e_{ij}. To meet the practical situation, every capacity of e_{ij} is denoted as x_{ij} for $1 \le i \le n-1$, $2 \le j \le n$ where $i \ne j$. A current capacity vector of each edge is denoted as $X = (x_{11}, x_{12}, \cdots, x_{n-1,n})$. Such a G obeys the subsequent assumptions:

(i) Every node is perfectly reliable.

(ii) All flows in G must satisfy the flow conservation law [35].

(iii) The capacities of the different edges are statistically independent.

(iv) The capacity of each edge e_{ij} is a random integer value which takes values from $\{0,1,2,\cdots,m_{ij}\}$ according to a given distribution.

Assumption (i) is necessary to ensure that each node will not fail. In fact, many existing studies have already moved away from this assumption. In the network description, node attributes are added. In the state description, state equations for the nodes are introduced. However, these additions do not constitute any fundamental changes to the underlying model. The flow conservation law in Assumption (ii) makes sure the amount of flow on each MP can be identified. Assumption (iii) is necessary for applying algorithms, such as the inclusion-

exclusion principle [36] and the sum of disjoint products [34], to calculate network reliability.

2.2. Network reliability

Given Z MPs of an SFN G, $MP_1, \cdots, MP_h, \cdots, MP_z$ can be obtained [37]. All feasible flow vectors $F = (f_1, \cdots, f_h, \cdots, f_z)$ can be derived from the following constraints in Eq.(1) via the implicit enumeration approach [38], where f_h is the MP that can flow successfully from the source s to sink t.

$$\begin{gathered} f_1 + \cdots + f_h + \cdots + f_z = d \\ f_h \le min\{M_{ij} | e_{ij} \in MP_h\}, for\ h = 1,2, \cdots, z \\ \sum_{h=1}^{t} \{f_h | e_{ij} \in MP_h\} \le M_{ij}, where\ i \ne j, for\ 1 \le i \\ \le n-1, 2 \le j \le n \end{gathered} \quad (1)$$

Each F can be transformed into an $X = (x_{11}, x_{12}, \cdots, x_{n-1,n})$, a d -MP candidate [29], via:

$$x_{ij} = \sum_{h=1}^{t} \{f_h | e_{ij} \in MP_h\}, where\ i \ne j, for\ 1 \le i \le n-1, 2 \le j \le n \quad (2)$$

Suppose q d -MP candidates, denoted as $\{X_1, X_2, \cdots, X_q\}$, are generated satisfying the constraints Eqs.(1)-(2). According to the theorem proposed by Yeh et al. [38], all d -MPs can be obtained by removing the non-minimal ones from these candidates.

Assume $\tilde{X}_1, \tilde{X}_2, \cdots, \tilde{X}_\theta$ are all d -MPs. Then, let $R_1 = \{X | X \ge \tilde{X}_1\}$, $R_2 = \{X | X \ge \tilde{X}_2\}$, …, $R_\theta = \{X | X \ge \tilde{X}_\theta\}$. The network reliability of the G can be formulated as follows:

$$R_d = Pr(R_1 \cup R_2 \cup \cdots \cup R_\theta) \quad (3)$$

2.3. 2-additive Choquet integral

The 2-additive Choquet integral [39] simplifies the expression of the general Choquet integral into:

$$f_\mu(x_1, \cdots, x_n) = \sum_{j=1}^{n} I_j x_j - \frac{1}{2} \sum_{j,k \in C} I_{jk} |x_j - x_k| \quad (4)$$

Here, μ is a 2-additive capacity. I_j is the Shapley index denoting the relative importance of each elementary criteria to all others. I_{jk} represents the mutual interaction between the indices x_j and x_k, which ranges in $[-1,1]$.

2.4. Interval-valued intuitionistic hesitant fuzzy vectors

Let X be a fixed set. An interval-valued intuitionistic hesitant fuzzy vector (IVIHFV) on X is defined in terms of a function that returns a subset of the set of all interval-valued intuitionistic fuzzy numbers when applied to X [40]. Mathematically, an IVIHFV is expressed as:

$$IVIHFV_x = \{(\gamma_x, \upsilon_x) | x \in X\} = \{([\gamma_x^-, \gamma_x^+], [\upsilon_x^-, \upsilon_x^+]) | x \in X\} \quad (5)$$

where γ_x and υ_x indicate the possible membership degree intervals and non-membership degree intervals of the element $x \in X$.

3. Networked modeling of CMSs

3.1. System structure analysis

From the perspective of logical structure, CMSs can be partitioned into multiple layers [41]. Each layer is characterized by a single core task and a unique type of connection. Furthermore, conditional dependencies exist between layers. Fig. 1 presents a schematic diagram of a three-layer structure for the CMS. From top to bottom, it comprises an electrical layer for power supply (Layer 1), a control layer for transmitting control commands (Layer 2), and an executive layer for executing prescribed actions (Layer 3). The electrical layer serves as the foundation, providing power to the components in both the control and executive layers; the control layer acts as the core, controlling the components in the executive layer to enable the completion of specified movements; and the executive layer serves as the ultimate executor of actions. In addition, the control layer is designed to facilitate the command and data transmission between specific components, utilizing a single type of informational connection. It is noteworthy that while the hierarchical depth may vary across different CMSs, the proposed modeling approach remains universally applicable.

To ensure data accessibility while mitigating the risk of combinatorial explosion, the components defined in this study are typically assemblies of multiple sub-parts or specific devices, which are referred to as MMUs in some literature.

3.2. System functional analysis

From the perspective of the SFNs, the implementation of dynamic functions in CMSs can be regarded as the transmission of various commodities with specified demand quantities from designated source nodes to sink nodes. Within this framework, each layer involves the transmission of specific demands between multiple source-sink node pairs. For example, during the traction process of an urban rail train system in Fig. 2, electricity is first distributed from the pantograph to other downstream components within the electrical layer. Subsequently, control commands are transmitted from the console to the traction motors within the control layer. Finally,

the traction force of a specified magnitude generated by the traction motors is transmitted to the wheelsets within the executive layer to propel the train. Furthermore, the capacity of the edges used for commodity transmission varies according to material types and operating time, thereby exhibiting multi-state characteristics.

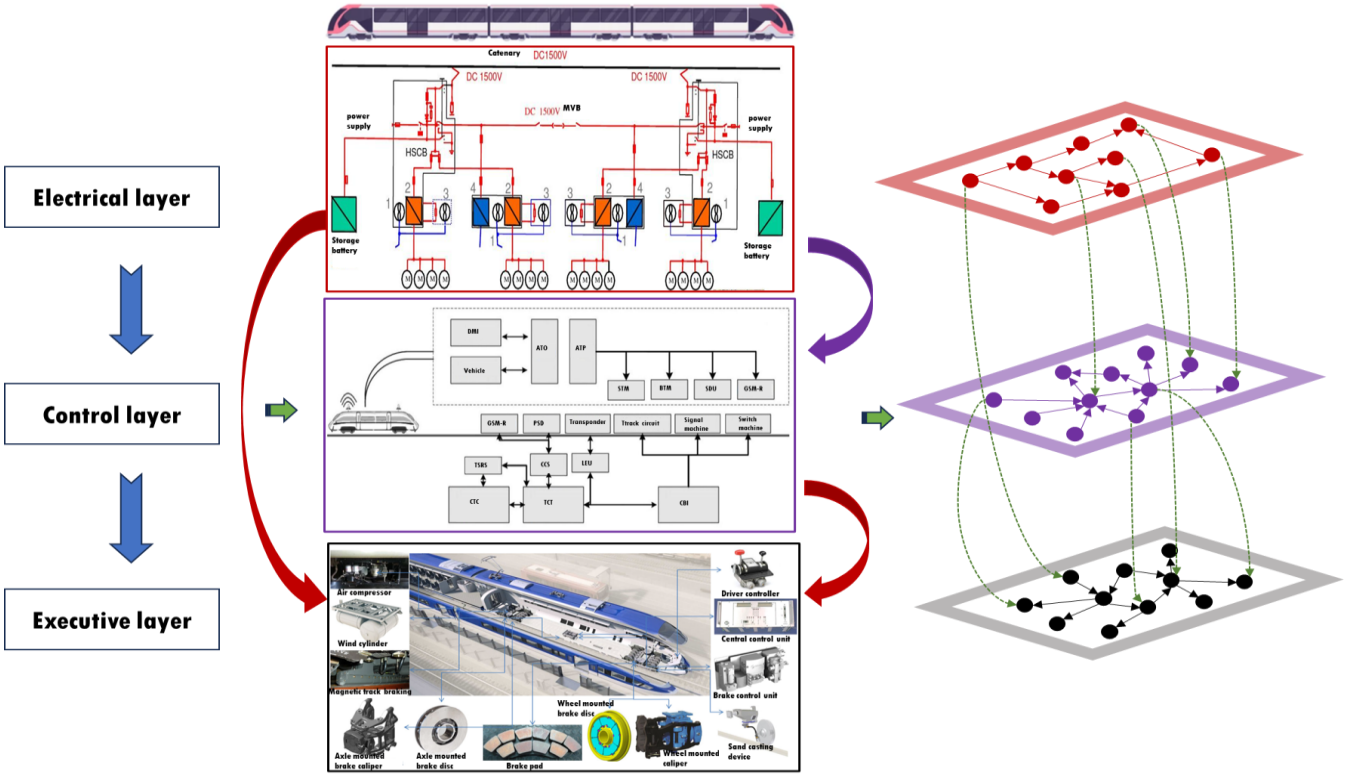

Figure 1. An example of the CMS.

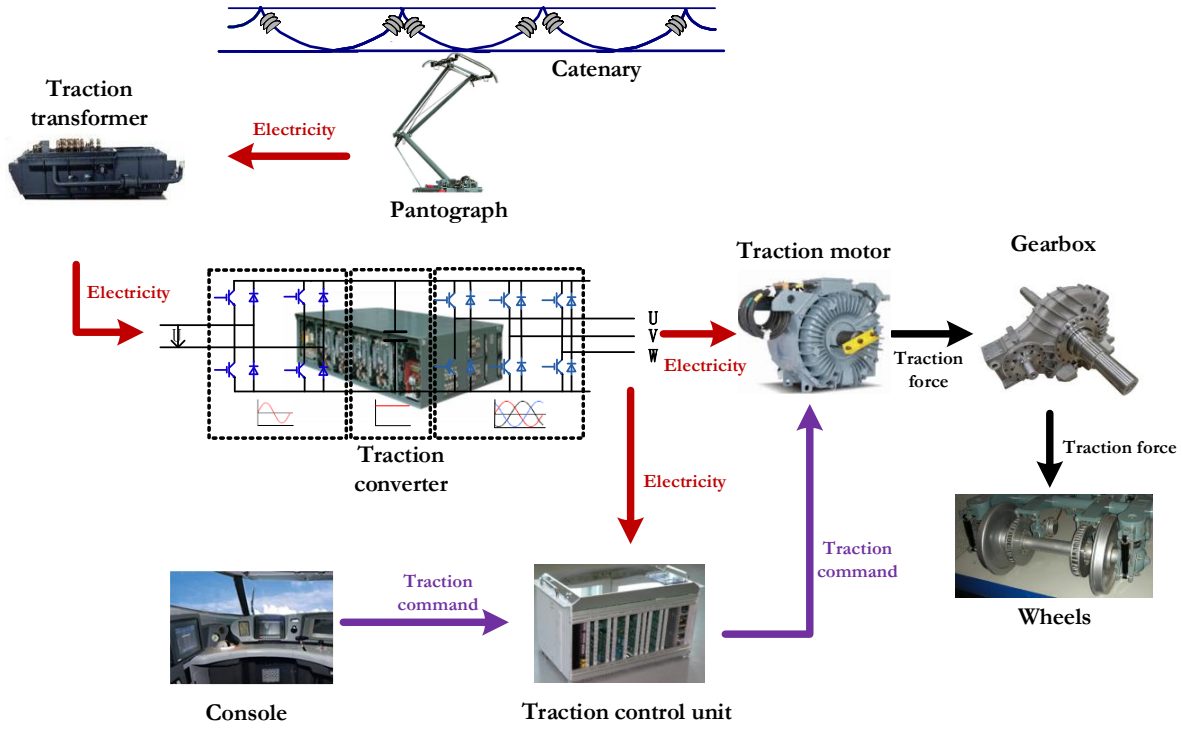

Figure 2. The traction process of an urban rail train system.

In addition, CMSs typically possess multiple functions, some of which can be executed concurrently, while others are mutually exclusive. Taking urban rail train system as an example, the traction and braking functions are mutually exclusive, whereas the broadcasting and air-conditioning functions can be performed simultaneously. By integrating the functions of the CMS, H mutually exclusive system functions are extracted

3.3. Construction of the MSFN

Based on the aforementioned characteristics, the CMS can be abstracted into a multi-layer stochastic flow network (MSFN). In this model, nodes and edges denote the system's topological structure, commodity flows describe its system functions, and edge attributes capture the multi-state characteristics of this system. The MSFN is formally defined by the triplet:

$$MSFN \equiv (G, D, \Gamma)$$
$$\begin{cases} G = \{G_L(V_L, E_L, C_L, W_L) | L = 1, \cdots, F\} \\ D = \{(OD_h, D_h) | h = 1, \cdots, H\} \\ \Gamma = \left\{E_{\alpha\beta} \subseteq V_\alpha \times V_\beta | \alpha, \beta \in L, \alpha \neq \beta\right\} \end{cases} \quad (6)$$

The element G represents the topology of the MSFN, where G_L denotes the topology of the L -th layer for the MSFN, defined by a quadruple. Let F indicate the total number of layers. For example, in Fig. 1, $L = 1,2,3$ correspond to the electrical layer, control layer, and executive layer, respectively. $V_L = \{v_i^L | i = 1, \cdots, n_L\}$ is the set of nodes in G_L, where v_i^L represents the i -th node, and n_L denotes the total number of nodes in G_L. Theoretically, G_L should contain all n components. However, since specific connection types may not exist between certain components within a given layer, isolated nodes may arise. To simplify the MSFN, these isolated nodes are removed, hence $n_L \leq n$.

$E_L = \left\{e_{i-j}^L \; or \; a_k^L | v_i^L, v_j^L \in V_L\right\}$ is the set of edges in G_L, where e_{i-j}^L denotes a directed edge of a specified type from node v_i^L to v_j^L within the L -th layer. To facilitate subsequent system reliability modeling, edges in G_L are re-indexed sequentially, and the alternative notation a_k^L represents the k -th edge in E_L. $C_L = \left\{c_{i-j}^L \; or \; c_{k_L}^L | e_{i-j}^L \in E_L, a_k^L \in E_L\right\}$ denotes the set of maximum capacities of edges in G_L, where c_{i-j}^L (or $c_{k_L}^L$) corresponds to the maximum capacity of the edge e_{i-j}^L (or a_k^L).

$W_L = \left\{w_{i-j}^{q_L^h} \; or \; w_{k_L}^{q_L^h} | q_L^h = 1,2, \cdots, p_L^h; h = 1, \cdots, H; e_{i-j}^L \in E_L, a_k^L \in E_L\right\}$ represents the flow consumed by each edge in G_L when transmitting different types of commodities, where $w_{i-j}^{q_L^h}$ (or $w_{k_L}^{q_L^h}$) is the flow consumed by the edge e_{i-j}^L (or a_k^L) while transmitting the q_L^h -th commodity. Finally, p_L^h is the total number of commodity types to be transmitted in G_L.

The element D describes the set of source-sink node pairs, along with the corresponding commodity types and demand quantities required to realize system functions. $OD_h = \left\{OD_{L,s}^h | h = 1, \cdots, H; L = 1, \cdots, F; s = 1, \cdots, n_L^h\right\}$ lists the set of specific source-sink pairs that require commodity transmission for the h -th system function, where $OD_{L,s}^h = \left(v_{O_s^h}^L, v_{D_s^h}^L\right)$ represents the s -th node pair in G_L, comprising the source node $v_{O_s^h}^L$ and the sink node $v_{D_s^h}^L$. For notational clarity, the identifiers $v_{O_s^h}^L$ and $v_{D_s^h}^L$ are introduced to replace the original node indices, with subscripts O_s^h and D_s^h explicitly distinguishing between source and sink roles in G_L for the h -th system function. n_L^h denotes the total number of source-sink pairs in G_L for the h -th system function.

$$D_h = \left\{d_{OD_{L,s}^h}^{q_L^h} | h = 1, \cdots, H; s = 1, \cdots, n_L^h; L = 1, \cdots, F; q_L^h = 1, \cdots, p_L^h\right\}$$

defines the set of demands quantities of each source-sink pair for every commodity type for the h -th system function, where $d_{OD_{L,s}^h}^{q_L^h}$ is the specific demand of the s -th source-sink pair for the q_L^h-th commodity and p_L^h represents the total number of types of commodities in G_L.

The element Γ represents the set of edges connecting different layers, referred to as virtual edges. Due to the inherent structural and functional complexity of CMSs, multiple types of connections may coexist between two components. However, since G_L is characterized by a single, specific connection modality, the same physical component may be mapped to separate nodes across different layers. To integrate these representations, virtual edges are introduced to connect nodes representing the same components in different layers, as illustrated by the green directed dashed lines in Fig. 1. $E_{\alpha\beta} = \left\{e_{v_i^\alpha - v_i^\beta} | v_i^\alpha \in V_\alpha, v_i^\beta \in V_\beta; \alpha, \beta \in L, \alpha \neq \beta\right\}$ denotes the set of virtual edges between G_α and G_β, where $e_{v_i^\alpha - v_i^\beta}$ represents a virtual edge connecting node v_i^α in G_α to node v_i^β in G_β.

4. System reliability model for management decisions

4.1. Layer reliability assessment

In the MSFN, the distinction between different system functions is primarily manifested by variations in the types of

commodities and demands required for transmission, while the underlying topological structure remains invariant. Consequently, the sub-network corresponding to the -th system function is extracted and denoted as:

$$MSFN_h \equiv (G_h, D_h, \Gamma)$$
$$\begin{cases} G_h = \{G_L^h(V_L, E_L, C_L, W_L^h) | L = 1, \cdots, F\} \\ D_h = \{D_L^h = (OD_L^h, D_L^h) | L = 1, \cdots, F\} \\ \Gamma = \left\{E_{\alpha\beta} \subseteq V_\alpha \times V_\beta | \alpha, \beta \in L, \alpha \neq \beta\right\} \end{cases} \quad (7)$$

where:

$W_L^h = \left\{w_{i-j}^{q_L^h} \text{ or } w_{k_L}^{q_L^h} | q_L^h = 1,2,\cdots,p_L^h; e_{i-j}^L \in E_L, a_k^L \in E_L\right\}$, $OD_L^h = \left\{OD_{L,s}^h = \left(v_{O_s^h}^L, v_{D_s^h}^L\right) | L = 1,\cdots,F; s = 1,\cdots,n_L^h\right\}$, and $D_L^h = \left\{d_{OD_{L,s}^h}^{q_L^h} | s = 1,\cdots,n_L^h; L = 1,\cdots,F; q_L^h = 1,\cdots,p_L^h\right\}$. Let $M_L^h = (G_L^h, D_L^h)$ represent the L -th layer of the $MSFN_h$, which is a multi-source multi-sink multi-commodity stochastic flow network (M3SFN). Compared to general SFNs, M_L^h is distinguished by its complex topology, featuring multiple source-sink node pairs and a wide variety of transmitted commodities. The reliability of this layer, referred to as layer reliability, is defined as the probability that all specified commodity types are successfully transmitted between their respective source-sink node pairs within the M_L^h, satisfying the prescribed demand requirements. Currently, few established reliability assessment models exist for such SFNs with these specific characteristics. Consequently, this paper proposes a layer reliability assessment method based on minimal paths (MPs).

The nodes are still assumed to be perfectly reliable in this study. While nodes are assumed to be perfectly reliable to simplify the network topology, this does not limit the ability of the model to represent real world component failures. In a physical context, any failure of a junction or a connecting component can be mathematically mapped onto its adjacent edges by reducing their capacities to zero. This ensures that the flow-based reliability assessment remains robust. In addition, it can also reduce the complexity of the state equations. Sensitivity analysis indicates that the output of the model is sensitive to how these mappings are defined. Therefore, assuming that the failure logic of physical entities is accurately integrated into the edge capacity distributions, and then treating nodes as perfectly reliable is a standard simplification in SFNs.

According to the principle of flow conservation, the layer state of M_L^h must satisfy the following three conditions: (i) Flow balance constraints. Flow conservation must be maintained for all source nodes, sink nodes and intermediate nodes within the M_L^h, i.e., Eqs.(8a)-(8b). (ii) Edge capacity constraints. The aggregated capacity consumption of all commodities traversing a specific edge must not exceed its maximum capacity, i.e., Eqs.(8c)-(8e). (iii) Physical constraints. Node capacity limits (if applicable) and flow non-negativity constraints must be strictly observed, i.e., Eq.(8f). Accordingly, the layer state equations are formulated as follows:

$$\sum_{i\neq j} x_{i-j}^{q_L^h}(OD_{L,s}^h) = \sum_{i\neq h} x_{u-i}^{q_L^h}(OD_{L,s}^h),\ v_i^L, v_j^L, v_u^L \notin \left\{v_{O_s^h}^L, v_{D_s^h}^L\right\}; q_L^h = 1,2,\cdots,p_L^h; s_L^h = 1,\cdots,n_L^h \quad (8a)$$

$$\sum_{i\neq j} x_{i-j}^{q_L^h}(OD_{L,s}^h) = \sum_{h\neq g} x_{u-g}^{q_L^h}(OD_{L,s}^h) = d_{OD_{L,s}^h}^{q_L^h},\ v_i^L = v_{O_s^h}^L; v_g^L = v_{D_s^h}^L; q_L^h = 1,2,\cdots,p_L^h; s_L^h = 1,\cdots,n_L^h \quad (8b)$$

$$\sum_{q_L^h=1}^{p_L^h} \sum_{s_L^h=1}^{n_L^h} x_{k_L}^{q_L^h}(OD_{L,s}^h) \le c_{k_L}^L, k_L = 1,\cdots,m_L \quad (8c)$$

$$\sum_{q_L^h=1}^{p_L^h} w_{k_L}^{q_L^h} \sum_{s_L^h=1}^{n_L^h} x_{k_L}^{q_L^h}(OD_{L,s}^h) \le c_{k_L}^L, k_L = 1,\cdots,m_L; w_{a_k^L}^{q_L^h} \ge 1 \quad (8d)$$

$$x_{i-j}^{q_L^h}(OD_{L,s}^h) \le d_{OD_{L,s}^h}^{q_L^h},\ v_i^L, v_j^L \notin \left\{v_{O_s^h}^L, v_{D_s^h}^L\right\}; q_L^h = 1,2,\cdots,p_L^h; s_L^h = 1,\cdots,n_L^h \quad (8e)$$

$$x_{i-j}^{q_L^h}(OD_{L,s}^h) = x_{k_L}^{q_L^h}(OD_{L,s}^h) \ge 0, v_i^L \neq v_j^L \in V_L; q_L^h = 1,2,\cdots,p_L^h; s_L^h = 1,\cdots,n_L^h; k_L = 1,\cdots,m_L \quad (8f)$$

where $x_{i-j}^{q_L^h}(OD_{L,s}^h)$ represents the capacity level on the k -th edge a_k^L when the q_L^h-th commodity is transmitted from source node $v_{O_s^h}^L$ to sink node $v_{D_s^h}^L$ within M_L^h.

Solving the above equations yields the set of all possible layer states, denoted by $P_L^h = \left(X_{L,1}^h; \cdots; X_{L,s_L^h}^h; \cdots; X_{L,\delta_L^h}^h\right)$, where $X_{L,s_L^h}^h = \left(x_1^1(OD_{L,1}^h), \cdots, x_1^{q_L^h}\left(OD_{L,n_L^h}^h\right), \cdots, x_{k_L}^1(OD_{L,1}^h), \cdots, x_{k_L}^{q_L^h}\left(OD_{L,n_L^h}^h\right)\right)$ represents the s_L^h-th layer state vector. Let the $D_{OD_L^h}^{p_L^h}$-MP represent the set of minimal paths for M_L^h under the source-sink pair OD_L^h and the demand p_L^h. The $D_{OD_L^h}^{p_L^h}$-MP candidates are the intermediate, potentially redundant state vectors generated by the algorithm.

Specifically, each layer state vector $X_{L,s_L^h}^h$ serves as a candidate. Subsequently, by applying the loop-free theorem proposed by Yeh et al. [38], the actual $D_{OD_L^h}^{p_L^h}$-MPs are obtained by filtering out non-minimal ones. Finally, the layer reliability is calculated as the probability of the union of all identified $D_{OD_L^h}^{p_L^h}$-MPs.

$$R_L^h = Pr\left(\left\{\bar{X}|X_{L,\delta_L^h}^h \le \bar{X}\ for\ all\ D_{OD_L^h}^{p_L^h} - MP\ X_{L,\delta_L^h}^h \in X_{D_{OD_L^h}^{p_L^h}}^h\right\}\right) = Pr\left(\left\{\bar{X}|X_{L,1}^h \le \bar{X}\right\} \cup \cdots \cup \left\{\bar{X}|X_{L,\delta_L^h}^h \le \bar{X}\right\} \cup \cdots \cup \left\{\bar{X}|X_{L,r_L^h}^h \le \bar{X}\right\}\right) = Pr\left(\cup_{\delta_L^h=1}^{r_L^h} X_{L,\delta_L^h}^h\right) \quad (9)$$

where

$$Pr\left\{\bar{X} = \left(\bar{x}_1^L, \bar{x}_2^L, \cdots, \bar{x}_{m_L}^L\right)|X_{L,\delta_L^h}^h = \left(\sum_{q_L^h=1}^{p_L^h} x_{1,q_L^h}^{\delta_L^h}, \cdots, \sum_{q_L^h=1}^{p_L^h} x_{k_L,q_L^h}^{\delta_L^h}, \cdots, \sum_{q_L^h=1}^{p_L^h} x_{m_L,q_L^h}^{\delta_L^h}\right) \le \bar{X} = \left(\bar{x}_1^L, \bar{x}_2^L, \cdots, \bar{x}_{m_L}^L\right)\right\} = \prod_{k_L=1}^{m_L} Pr\left\{\sum_{q_L^h=1}^{p_L^h} \sum_{s_L^h=1}^{n_L^h} x_{i-j}^{q_L^h}(OD_{L,s}^h) \le \bar{x}_{k_L}^L\right\} \quad (10)$$

4.2. Local reliability analysis

The realization of each system function necessitates the sequential fulfillment of prescribed tasks by all layers. Consequently, the local reliability is defined as the degree of completion for each individual system function. From the perspective of the MSFN, the local reliability of the h -th system function can be viewed as the reliability of the sub-network $MSFN_h$. The local reliability is determined by the layer reliability for all layers and the relationships between layers. Considering the conditional dependencies between layers, the local reliability is defined as:

$$R_h = \otimes\left(R_1^h, \cdots, R_L^h, \cdots, R_F^h\right) \quad (11)$$

where $\otimes$ is the layer operator, representing the relationships between different layer reliabilities.

As detailed in Section 3.1, the same component may appear in different layers simultaneously and the presence of inter-layer conditional dependencies imply that layer reliabilities are statistically dependent. To address this, the 2-additive Choquet integral in Eq.(4) is selected as the layer operator due to its capability to model pairwise interactions between attributes. Consequently, the local reliability is updated as:

$$R_h = \sum_{i=1}^{F} I_i R_i^h - \frac{1}{2}\sum_{j=1}^{F} I_{ij}\left|R_i^h - R_j^h\right| \quad (12)$$

where I_i is the Shapley value of R_i^h, and I_{ij} is the interaction index between R_i^h and R_j^h, representing their interaction relationship, including positive cooperation, negative cooperation, and mutual independence.

Existing studies typically employ the Mahalanobis-Taguchi System (MTS) to compute the Shapley value I_i [42]. Unlike other approaches [43,44], the MTS method captures both the relative importance of a single attribute from a local perspective and the variations in subset importance from a global perspective. Fig. 3 illustrates the process of calculating I_i using the MTS.

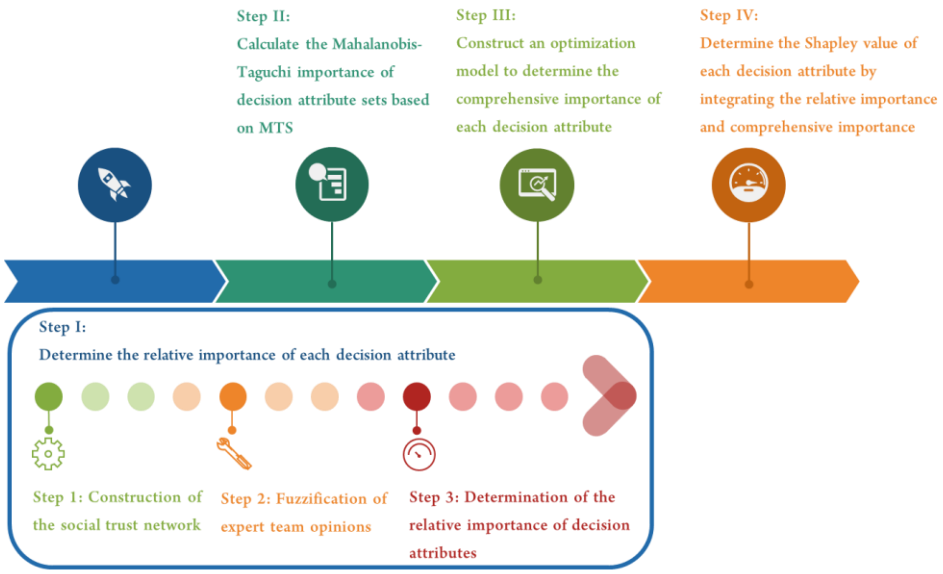

Figure 3. Process of computing the Shapley value I_i.

However, the relative importance of decision attributes (i.e., layer reliability for all layers) in *Step I* in Fig. 3 is conventionally determined using the analytic hierarchy process (AHP). For CMSs with intricate functional structures, relying

solely on a single expert's opinion to derive these weights is inadequate and prone to subjectivity. Therefore, on the basis of existing MTS-based Shapley value calculation methods, this paper proposes a novel approach for determining the relative weights of decision attributes using social networks and interval fuzzy sets in Fig. 3. The specific steps are as follows:

Step 1: Construction of the social trust network.

First, an expert panel is established, comprising m experts selected from various departments within the CMS domain. Based on their mutual trust relationships, a social trust network (STN) is constructed. Let $STN = (EX, RL)$ denote this network, where $EX = \{ex_1, \cdots, ex_r, \cdots, ex_m\}$ represents the set of nodes, with ex_r denoting the r -th expert in this team. $RL = \{rl_{ij} | ex_i, ex_j \in EX\}$ represents the set of directed arcs, where the existence of an edge rl_{ij} signifies that expert ex_i trusts expert ex_j. By incorporating the degree centrality measure [45], the trust degree of expert ex_r toward expert ex_h is defined as follows:

$$TC_{rh} = \frac{CC_{rh}}{d_{out}(ex_r)+d_{in}(ex_h)-2-CC_{rh}} \quad (13)$$

where $d_{out}(ex_r) = \sum_{t=1}^{m} a(ex_r, ex_t)$ and $d_{in}(ex_h) = \sum_{t=1}^{m} a(ex_t, ex_h)$ represent the out-degree of node ex_r and the in-degree of ex_h, respectively. The value of $a(ex_r, ex_t)$ is 1 or 0. $a(ex_r, ex_t) = 1$ if a connection exists between node ex_r and ex_t, and $a(ex_r, ex_t) = 0$ otherwise. CC_{rh} is the number of experts commonly trusted by both ex_r and ex_h, measured by the number of mutually recognized experts [44].

Within the STN, a higher level of trust is vested in an expert with greater authority, thereby justifying a larger weight assignment for their opinion. Consequently, the expert weight is formulated as:

$$w_r = \frac{TC_r}{\sum_{h=1}^{m} TC_h} = \frac{\frac{1}{m-1}\sum_{h=1}^{m} TC_{hr}}{\sum_{h=1}^{m}\frac{1}{m-1}\sum_{j=1}^{m} TC_{jh}} \quad (14)$$

where TC_r represents the trust level of other experts toward expert ex_r.

Step 2: Fuzzification of expert team opinions.

Initially, let $A = \{R_i^h | i = 1, \cdots, F\}$ denote the set of decision attributes. The subjective importance assigned to the i -th attribute by expert ex_r is denoted as $EI_{ri} \in [0,1]$. It is acknowledged that subjective assessments are often susceptible to deviation, such as bias toward higher or lower values. A key premise is that the precision of an opinion is positively correlated with the expert's authority. Specifically, the higher the authority of the expert, the smaller the associated error margin. To account for the inherent hesitancy and cognitive uncertainty in expert judgments, the IVIHFVs in Eq.(5) are introduced to model these opinions. Consequently, based on the initial subjective importance EI_{ri}, the IVIHFV representing each expert's opinion is constructed as follows:

$$IVIHFV_{ri} = ([\gamma_{ri}^-, \gamma_{ri}^+], [\upsilon_{ri}^-, \upsilon_{ri}^+]) = ([EI_{ri} - (1-w_r)\xi, EI_{ri} - (1+w_r)\xi], [1 - EI_{ri} + (1-w_r)\xi, 1 + EI_{ri} - (1-w_r)\xi]) \quad (15)$$

where $[\gamma_{ri}^-, \gamma_{ri}^+]$ is the range of importance for the i -th decision attribute given by expert ex_r, while $[\upsilon_{ri}^-, \upsilon_{ri}^+]$ represents the range of impossible values. ξ represents the hesitancy degree associated with the expert's judgment.

Combined with the interval-valued intuitionistic hesitant fuzzy Choquet integral (IVIHFCI) operator [46], the comprehensive IVIHFVs of the i -th decision attribute, denoted as EIF_i, can be obtained by aggregating the IVIHFVs of m experts for the i -th decision attribute.

$$EIF_i = IVIHFCI_i(EIF_{1i}, \cdots, EIF_{mi}) = \left(\left[\prod_{j=1}^{m} \left(\gamma_{(j)i}^-\right)^{w_{(j)}-w_{(j-1)}}, \prod_{j=1}^{m} \left(\gamma_{(j)i}^+\right)^{w_{(j)}-w_{(j-1)}} \right], \left[1 - \prod_{j=1}^{m} \left(\upsilon_{(j)i}^-\right)^{w_{(j)}-w_{(j-1)}}, 1 - \prod_{j=1}^{m} \left(\upsilon_{(j)i}^+\right)^{w_{(j)}-w_{(j-1)}} \right] \right) \quad (16)$$

where $\gamma_{(j)i}^-$ refers to the j -th largest value among all γ_{ri}^- values provided by the experts.

Step 3: Determination of the relative importance of decision attributes.

Given the superiority of the Hamming distance in handling discrete data [47], it is adopted herein to compute the relative importance of the i -th decision attribute, which is expressed as:

$$w_i^C = \frac{d(EIF_i, \alpha^+)}{d(EIF_i, \alpha^+)+d(EIF_i, \alpha^-)} \quad (17)$$

where:

$$d(EIF_i, \alpha^+) = \frac{1}{4m}\sum_{j=1}^{m} (|\, max\, \gamma_{ji}^- - \gamma_{ji}^-| + |\, max\, \gamma_{ji}^+ - \gamma_{ji}^+| + |\, min\, \upsilon_{ji}^- - \upsilon_{ji}^-| + |\, min\, \upsilon_{ji}^+ - \upsilon_{ji}^+|)$$

$$d(EIF_i, \alpha^-) = \frac{1}{4m}\sum_{j=1}^{m} (|\, min\, \gamma_{ji}^- - \gamma_{ji}^-| + |\, min\, \gamma_{ji}^+ - \gamma_{ji}^+| + |\, max\, \upsilon_{ji}^- - \upsilon_{ji}^-| + |\, max\, \upsilon_{ji}^+ - \upsilon_{ji}^+|)$$

d is the Hamming distance. α^+ and α^- are the positive and negative ideal solution, respectively [47].

Given the known Shapley values I_i for each decision attribute, a multi-objective optimization model can be constructed with the objective function of maximizing the comprehensive attribute value of each decision alternative under the 2-additive Choquet integral to solve for the interaction index I_{ij} in Eq.(12) [42].

4.3. System reliability model

Based on the definition of the reliability, the system reliability of a CMS is defined as the completion degree of H mutually exclusive system functions under specified conditions and within a specified time frame, as illustrated in Fig. 4. Although system functions are mutually exclusive, the components responsible for executing these functions may be shared. Therefore, the system reliability is expressed as:

$$R = \perp (R_1, \cdots, R_h, \cdots, R_H) \tag{18}$$

where $\perp$ is the functional operator, representing the functional relationship between the H system functions and the overall system reliability. R_h denotes the local reliability of the h -th system function.

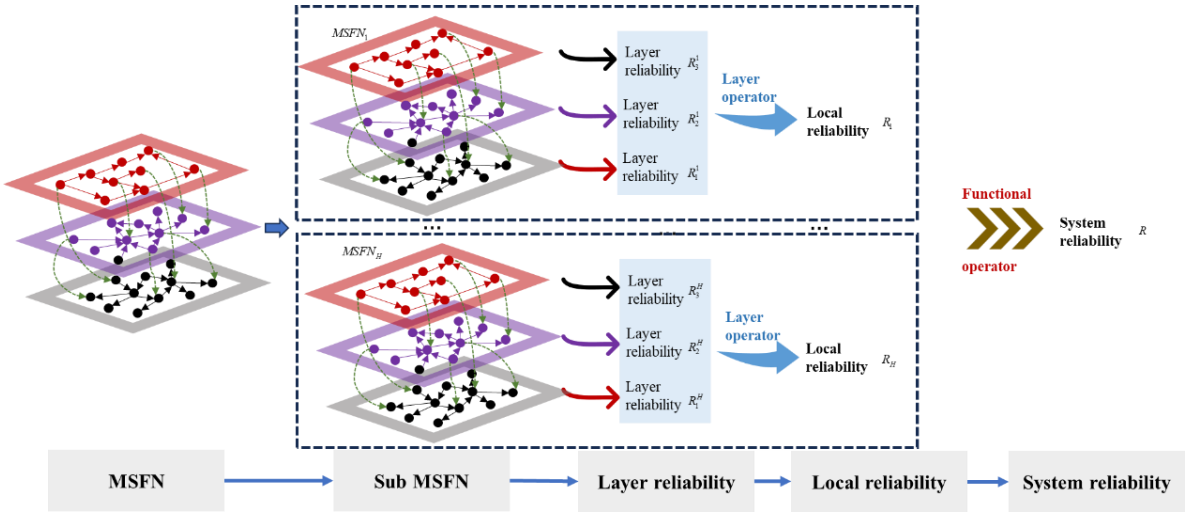

Figure 4. System reliability evaluation process.

The objective of reliability assessment for CMSs is to provide decision support for management. Depending on specific decision-making requirements, appropriate functional operators $\perp$ can be either selected or constructed. These three specific scenarios were deliberately selected as the primary focus because they comprehensively cover the most critical phases of the CMS lifecycle: design, critical operation, and routine maintenance. Specifically, Scenario II (reliability-cost trade-off) addresses the strategic planning and resource allocation requirements during the system design phase. Scenario I (emergency decision-making) captures the necessity for rapid, time-sensitive responses during the critical operational phase when sudden, cascading failures occur. Finally, Scenario III (maintenance decision-making) targets the scheduling and resource constraints inherent in the long-term operation and maintenance phase. Together, these three scenarios form a closed-loop management perspective, demonstrating the broad applicability of the proposed methodology across the core decision-making contexts faced by CMS management departments.

4.3.1. Scenario I: Emergency decision-making under sudden failures

Timeliness constitutes the primary constraint of emergency decision-making. As failure propagation is often measured in seconds or minutes, the system reliability model must overcome high computational latency to ensure immediate online assessment upon receiving fault alarms. Timeliness secures a critical decision-making window before an incident escalates, providing the essential temporal basis for determining preemptive intervention timing and for the formulation and execution of emergency strategies.

The focus of assessment in emergency scenarios shifts from maintaining the system's full-functional operation to ensuring the survival and ultimate accomplishment of core critical functions. System reliability assessment needs center on core

mission reliability, defined as the probability of the system completing safety-critical functions, such as braking control and trajectory maintenance, under specific constraints. For instance, by sacrificing comfort functions or partial non-core traction power, the probability of achieving core objectives (e.g., a train safely entering a station) is maximized, thereby realizing an optimal functional configuration under resource-constrained conditions.

In addition, sudden failures are frequently accompanied by data degradation induced by environmental noise, rendering deterministic reasoning inapplicable. Consequently, the output of system reliability assessment should not be limited to point estimates but must provide interval estimates incorporating confidence intervals. By quantifying epistemic uncertainty, the credibility of recommendations is explicitly defined.

Based on the above, the system reliability model under Scenario I is updated as follows:

$$R = \left[min\left(\bigcup_{i=1}^{H} \omega_i R_i, min_{i=1}^{H} R_i, \bigcup_{j\in\Lambda} R_j, min_{j\in\Lambda} R_j\right), max\left(\bigcup_{i=1}^{H} \omega_i R_i, min_{i=1}^{H} R_i, \bigcup_{j\in\Lambda} R_j, min_{j\in\Lambda} R_j\right)\right] \quad (19)$$

where ω_i represents the weight of the i -th system function and Λ is the set of critical system functions.

4.3.2. Scenario II: Reliability-cost trade-off decision-making

In reliability-cost trade-off decision-making, cost resources are finite. The system reliability should be capable of reflecting the importance of local reliability, thereby precisely identifying components within the system architecture that offer high cost-effectiveness ratios for improvement. For instance, upon identifying a functional module with high importance, the decision model should guide the prioritization of budgetary allocation toward it, rather than investing in redundant units with low importance, thus achieving Pareto optimization of resource configuration.

In the design phase, financial metrics can be directly incorporated into the system reliability model. System reliability should model it as a dependent variable driven by financial investment. Consequently, the system reliability model can consider acquisition costs and failure risk costs as core parameters. The former manifests as an investment function that grows exponentially with increasing reliability requirements, while the latter is described by an expected loss function that decreases monotonically with reliability improvements.

Given the iterative nature of CMS design, the system reliability model needs to bridge macro-performance indicators with micro-design parameters. System-level reliability thresholds and total budgets are scientifically allocated to various subsystems or functional modules to formulate design constraints. Concurrently, the final system reliability is inferred based on component specifications and topological logic. Through this bidirectional inference mechanism, optimal redundancy strategies and component specifications are determined, ensuring that the design scheme possesses both engineering feasibility and optimality while satisfying top-level metrics.

In summary, the system reliability model under Scenario II is expressed as:

$$R = \sum_i^H \left[\omega_i(\chi_i + \tau_i)R_i - \omega_j\left(\chi_j + \tau_j\right)R_j\right]g_{R_i} \quad (20)$$

where χ_i is the acquisition cost, τ_i is the failure risk cost for the i -th system function, and g_{R_i} is a fuzzy measure [41].

4.3.3. Scenario III: Maintenance decision-making

In maintenance decision-making for CMSs, the cost of downtime is prohibitive. As a critical metric, system reliability needs to account for the impact of maintenance duration. The central concern is whether the maintenance strategy can effectively restore system performance to operational requirements within a constrained time window.

Moreover, maintenance resource constraints are the core factors leading to the loss of statistical independence among components. When multiple independently failed components share limited maintenance crews or spare parts inventories, resource-induced stochastic dependence emerges within the system. Consequently, factors such as maintenance crew size and spare parts inventory levels should be explicitly incorporated into the system reliability model.

In reality, maintenance activities typically cannot restore a degraded equipment to its originally new state. Therefore, the system reliability model must account for the degree of component restoration. This allows for an accurate evaluation of how the repair depth influences the subsequent reliability degradation trajectory of the system.

The system reliability in Scenario III is improved as:

$$R = \oint_{i\in\Lambda}(rt_i \times rp_i \times sn_i \times R_i)dR_i \quad (21)$$

where $\oint$ is the Hamacher Choquet integral [48]. rt_i is the repair time ratio of the i -th system function. If the actual repair time for the i -th system function is less than the downtime window, rt_i equals 1. If it exceeds the downtime window, rt_i takes a value within the interval $(0,1)$, reflecting the degree to which the i -th system function is restored to the minimum operational performance requirements within that window.

rp_i denotes the maintenance personnel ratio of the i -th system function. If the actual number of maintenance personnel exceeds the specified minimum requirement, $rp_i = 1$. Otherwise, rp_i takes a value within the interval $(0,1)$, representing the proportion to which the actual maintenance crew can restore the system performance to the required standards.

sn_i is the spare parts ratio of the i -th system function. If the quantity of spare parts in stock $s\tilde{n}_i$ exceeds the actual demand $s\tilde{n}_i$, $s\tilde{n}_i$ takes a value of 1. Otherwise, it is the ratio of the actual demand to the quantity of spare parts in stock. Hence, sn_i is expressed as:

$$sn_i = \begin{cases} 1, s\tilde{n}_i \le s\tilde{n}_i \\ \frac{s\tilde{n}_i}{s\tilde{n}_i}, otherwise \end{cases} \quad (22)$$

5. Case study

5.1. The MSFN of the urban rail train system

Taking the urban rail train system as a case study, this paper selects two critical system functions to illustrate the proposed method, namely, the traction function and the braking function, which are denoted as h_1 and h_2, respectively. The two selected functions basically cover the components related to all train operational safety. 18 components related to traction and braking functions are extracted together with nine electrical connections, eight information connections, and seven mechanical connections. According to Section 3, the MSFN of the urban rail train system is constructed in Fig. 5, and for each system function $h_i(i = 1,2)$, the sub-network is extracted:

$$MSFN_{h_i} \equiv \left(G_{h_i}, D_{h_i}, \Gamma\right)$$

$$\begin{cases} G_{h_i} = \left\{G_L^{h_i}\left(V_L, E_L, C_L, W_L^{h_i}\right) | L = 1,2,3\right\} \\ D_{h_i} = \left\{D_L^{h_i} = \left(OD_L^{h_i}, D_L^{h_i}\right) | L = 1,2,3\right\} \\ \Gamma = \left\{E_{\alpha\beta} \subseteq V_\alpha \times V_\beta | \alpha, \beta \in L, \alpha \neq \beta\right\} \end{cases} \quad (23)$$

5.2. System reliability assessment

For the h_1-th system function, the layer state equations for the layer $M_1^{h_1}$ are constructed based on Eq.(8). All $D_{OD_1^{h_1}}^{p_1^{h_1}}$ -MP candidates can be obtained by solving Eq.(8) using the enumeration method, and all real $D_{OD_1^{h_1}}^{p_1^{h_1}}$-MPs can be calculated based on the loop-free theorem [38], as shown in Table 1. Then, by applying Eqs.(9)-(10) and the fast inclusion-exclusion method [34], the layer reliability of $M_1^{h_1}$ is determined to be $R_1^{h_1} = 0.9368$.

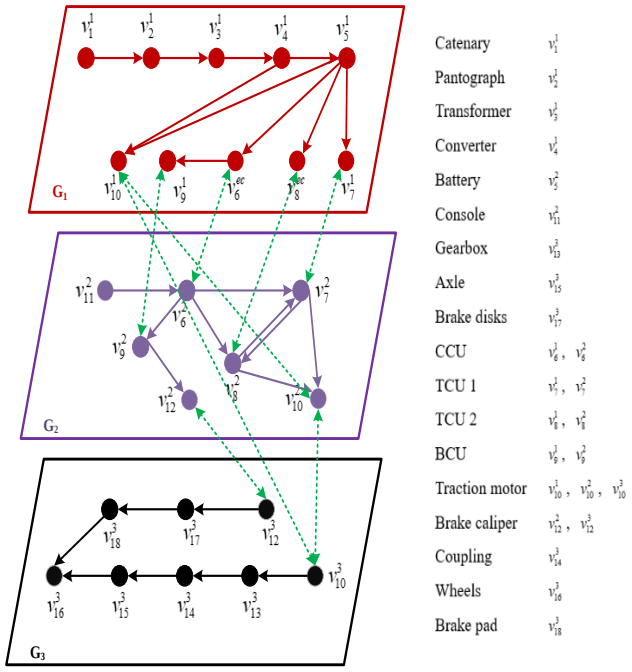

Figure 5. The MSFN of the urban rail train system.

By repeating the above steps, the layer reliability of the layer $M_2^{h_1}$ and $M_2^{h_1}$ for the h_1-th system function can be obtained as $R_2^{h_1} = 0.9422$ and $R_3^{h_1} = 0.9199$. In the same manner, the layer reliability for the h_2-th system function is $R_1^{h_2} = 0.9216$, $R_2^{h_2} = 0.9357$, and $R_3^{h_2} = 0.9401$, respectively.

As described in Section 4.2, an STN consisting of 20 experts in the field of rail transit is constructed, as illustrated in Fig. 6, where nodes denote experts and edges signify the trust relationships among them.

According to Eqs.(13)-(14), the expert weights are calculated as shown in Table 2.

Subsequently, the relative importance can be solved based on Eqs.(15)-(17), i.e., $w_1^C = 0.3429$, $w_2^C = 0.3012$ and $w_3^C = 0.3559$. According to Fig. 3, Shapley values I_i and interaction

indices I_{ij} can be calculated, as presented in Table 3. Based on Eq.(12), the local reliability is $R_{h_1} = 0.9249$ and $R_{h_2} = 0.9264$, respectively.

Table 1. $D_{OD_1^{h_1}}^{p_1^{h_1}}$-**MPs**.

	$X_{1,1}^{h_1,\delta_1^{h_1}} = \left(x_{1-2,1}^{\delta_1^{h_1}}; x_{2-3,1}^{\delta_1^{h_1}}; \cdots; x_{4-10,1}^{\delta_1^{h_1}}\right)$					…	$X_{1,5}^{h_1,\delta_1^{h_1}} = \left(x_{1-2,5}^{\delta_1^{h_1}}; x_{2-3,5}^{\delta_1^{h_1}}; \cdots; x_{4-10,5}^{\delta_1^{h_1}}\right)$		
$\delta_1^{h_1}$	$x_{1-2,1}^{\delta_1^{h_1}}$	…	$x_{3-4,1}^{\delta_1^{h_1}}$	…	$x_{4-10,1}^{\delta_1^{h_1}}$	…	$x_{1-2,5}^{\delta_1^{h_1}}$	…	$x_{4-10,5}^{\delta_1^{h_1}}$
1	(6,0,0,0)	…	(0,0,0,0)	…	(0,0,0,0)	…	(1,0,0,0)	…	(0,0,0,0)
2	(6,0,0,0)	…	(1,0,0,0)	…	(0,0,0,0)	…	(1,0,0,0)	…	(0,0,0,0)
3	(6,0,0,0)	…	(2,0,0,0)	…	(0,0,0,0)	…	(1,0,0,0)	…	(0,0,0,0)
4	(6,0,0,0)	…	(3,0,0,0)	…	(0,0,0,0)	…	(1,0,0,0)	…	(0,0,0,0)

Table 2. Expert weights.

w_1	w_2	w_3	w_4	w_5	w_6	w_7
0.0112	0.0763	0.0410	0.0585	0.0662	0.0662	0.0639
w_8	w_9	w_{10}	w_{11}	w_{12}	w_{13}	w_{14}
0.0967	0.0389	0.0431	0.0630	0.0343	0.0037	0.0752
w_{15}	w_{16}	w_{17}	w_{18}	w_{19}	w_{20}	
0.0432	0.0284	0.0363	0.1018	0.0456	0.0544	

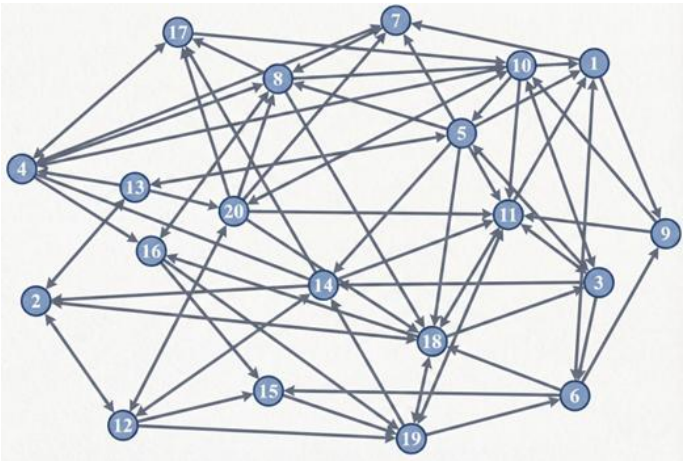

Figure 6. The STN in the field of rail transit.

Table 3. Shapley value and interaction indices.

Shapley value			Interaction indices		
I_1	I_2	I_3	I_{12}	I_{13}	I_{23}
0.3422	0.2955	0.3623	0.3478	0.304	0.3482

Considering the variations in operating moments, the probability of edges assuming the same capacity differs [31]. At $t = 3$ million running kilometers [41], the system reliability for Scenario I (emergency decision-making under sudden failures in Section 4.3.1) is calculated as an interval $R_{Scenario\ I} = [0.8484, 0.8568]$. The system reliability values for Scenario II (reliability-cost trade-off decision-making in Section 4.3.2) and Scenario III (maintenance decision-making in Section 4.3.3) are $R_{Scenario\ II} = 0.9257$ and $R_{Scenario\ III} = 0.9249$, respectively. The computational times corresponding to these three scenarios are 126 seconds, 139 seconds, and 177 seconds, respectively.

It is evident that Scenario I achieves the highest computational efficiency, whereas Scenario II exhibits a slower calculation speed. This observation aligns with the inherent trade-off between computational efficiency and accuracy, where an increase in speed typically entails a compromise in precision. Specifically, Scenario I prioritizes computational speed over precision. In contrast, Scenario II demands higher precision, necessitating a tolerance for lower calculation speeds. Scenario III, however, places equal importance on both precision and speed, aiming for a balanced performance.

Fig. 7 illustrates the system reliability of the three scenarios at different running times. It is evident that the system reliability in Scenario I is significantly lower than that in the other two scenarios. The fundamental reason is that the improvement in computational efficiency comes at the expense of some accuracy. For Scenario I, this trade-off is acceptable. It provides the potential worst-case outcome at the fastest computational speed, facilitating the formulation of flexible contingency plans. In contrast, the system reliability in Scenario II is significantly higher than that in the other two scenarios. The design phase typically prioritizes accuracy over computational speed, as high precision is beneficial for cost estimation. Scenario III is geared towards routine maintenance, imposing certain requirements on

both time and accuracy. Consequently, its reliability analysis results generally fall between those of the other two scenarios.

Furthermore, system reliability does not strictly decrease over time. This is attributed to the periodic maintenance of urban rail transit systems. Although system performance is enhanced following maintenance, it clearly does not reach the originally new state. This observation is consistent with practical engineering reality.

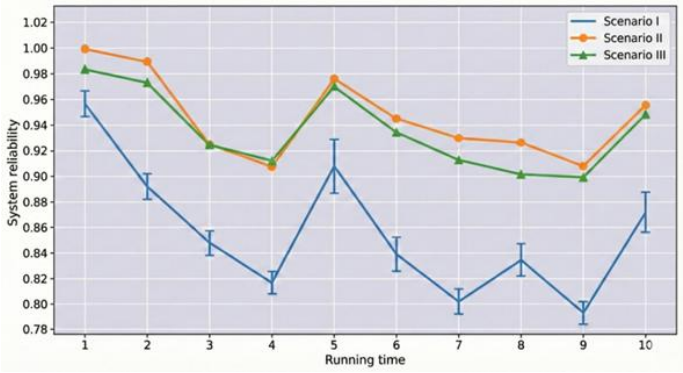

Figure 7. System reliability at different running time for three scenarios.

5.3. Discussion and analysis

As discussed, networking models serve as the cornerstone of system reliability assessment. To illustrate this, Fig. 8 presents two common network models found in existing research. Compared to the proposed MSFN, the single-layer network in Fig. 8(a) completely overlooks the heterogeneity of different types of connections. Besides, while the three-layer topological network in Fig. 8(b) accounts for node diversity, the distinct characteristics of connections between different node types are still ignored. Furthermore, both models fail to incorporate the dynamic characteristics of the system. In contrast, the proposed network in Fig. 5 simultaneously describes the overall system topology and the implementation process of dynamic functions, making it more suitable for comprehensive system reliability analysis.

In Section 4.2, this paper proposes using the relative importance to replace the decision attribute weights determined by a single expert's opinion in the traditional MTS approach for calculating Shapley values. Fig. 9 illustrates the urban rail train system reliability obtained after calculating the relative importance of decision attributes based on the opinions of experts with the highest and lowest weights, respectively. Based on the opinion of the high-weight expert (ex_{18}), the average difference between the system reliability obtained using this expert's opinion and the proposed method is approximately 0.002, whereas the average difference for the low-weight expert (ex_{13}) is approximately 0.1. Although the difference between the results based on authoritative expert opinions and the method in this paper is small, for an urban rail train system composed of more than 40,000 components, it is nearly impossible to find a single authoritative expert familiar with all aspects of the system. Additionally, while this paper only considers two system functions and the resulting gap between different weighting methods is small, this discrepancy will increase exponentially as the number of system functions grows. This underscores the criticality of establishing an expert team to determine the relative importance of attributes in system reliability analysis as proposed in this paper.

Fig. 10 presents the system reliability analysis of the urban rail train system under Scenario 2 following a single-node failure, using five different methods. Significant discrepancies exist between the results obtained by the proposed method and those measures, including topological reliability [22], functional reliability [23], comprehensive reliability [26], and task reliability [21] for certain nodes. For instance, after a failure at node v_1, the system reliability obtained by the proposed method is 0. Node v_1 provides power to the urban rail train system; if the power supply fails, the probability of the train performing any function becomes 0, resulting in a system reliability of 0. Similarly, the system reliability is also 0 after failures at nodes v_2 and v_3. This is because, during power supply tasks, the electricity generated by node v_1 can only be distributed to other nodes in the system through v_2 and v_3. Once they fail, the consequence is essentially the same as a failure at node v_1. The other four methods are primarily based on topological structures and ignore the dynamic functions of the system, thus yielding results greater than 0.

From a management decision-making perspective, selecting an appropriate reliability assessment method requires balancing modeling complexity, operational accuracy, and risk mitigation. Existing measures, including topological reliability, functional reliability, comprehensive reliability, and task reliability, are primarily based on topological structures and often ignore the dynamic functions of the system. While these methods may require less initial effort to model, they can produce overly

optimistic reliability estimates. For example, even when a critical power node fails and the entire system stops working, they still produce results greater than 0. Relying on these models can lead to misallocated maintenance crews and severely misinformed emergency response strategies. The proposed method involves a higher initial investment in constructing the MSFN and analyzing system functions. However, it equips operational managers with a decisive advantage by simultaneously characterizing the global topology and dynamic functional execution mechanisms. This enables highly accurate, scenario-specific predictions immediately following a single-node disruption, preventing false optimism and supporting agile, time-sensitive decision-making for emergency maintenance and dynamic flow rerouting, ultimately minimizing system downtime and operational losses.

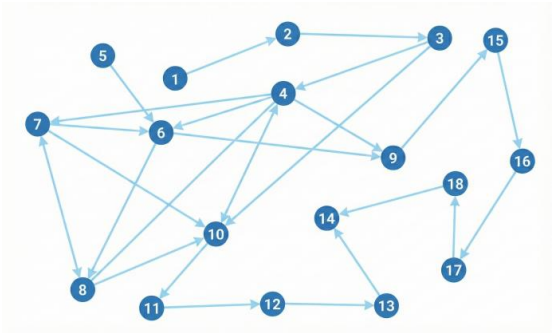

(a) The single network

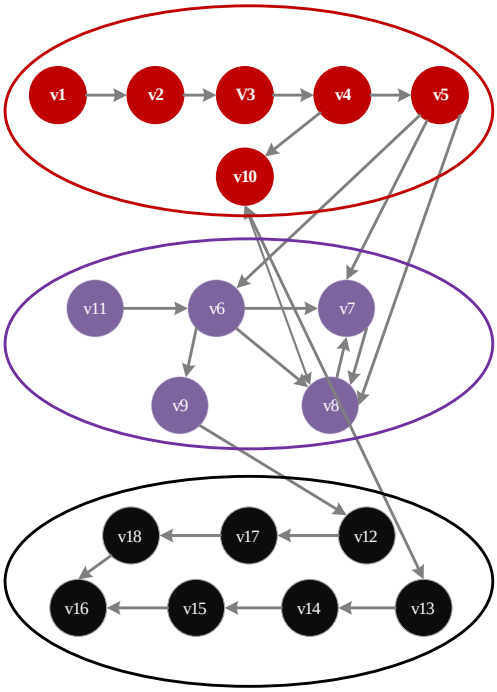

(b) Three-layer topological network

Figure 8. Topological network of the urban rail train system.

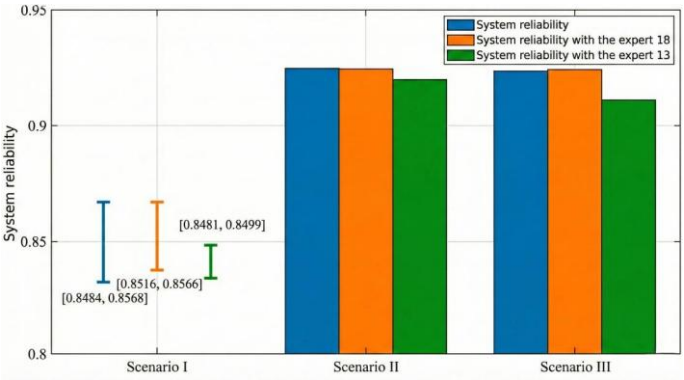

Figure 9. System reliability with different weights of decision attributes.

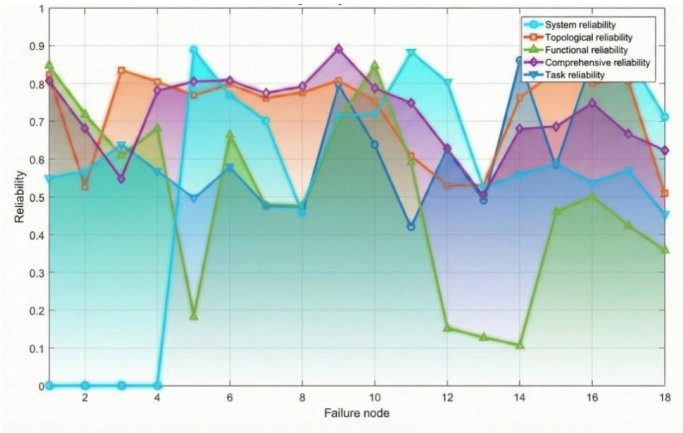

Figure 10. System reliability after a single-node failure.

To handle the potential combinatorial explosion in systems with a large number of components, such as exceeding 40,000, the proposed MSFN framework employs a hierarchical decomposition strategy. Instead of searching for MPs in a single, flat large-scale network, the system is partitioned into multiple functional layers and subsystems based on its physical and operational logic. This modular approach ensures that the number of nodes in each sub-network remains within a computationally manageable range. Furthermore, network simplification techniques, such as merging series-parallel components and pruning non-critical nodes, are applied during the pre-processing stage to further enhance computational efficiency without compromising assessment accuracy.

6. Conclusion

This paper proposes a reliability modeling method for CMSs based on MSFNs and fuzzy theory, addressing the limitations of existing research that often overlooks specific management decision requirements. The approach abstracts the CMS into an MSFN to simultaneously characterize its global topology and

dynamic functional execution. To assess reliability across the system hierarchy, the method utilizes MPs for layer reliability and the 2-additive Choquet integral as a layer operator to capture inter-layer dependencies for local reliability. Furthermore, to mitigate expert cognitive uncertainty and subjectivity, the framework integrates interval hesitant fuzzy sets and the MTS to solve for Shapley values and interaction indices.

The proposed framework establishes a progressive modeling path from layer reliability to system reliability through the use of functional operators tailored to diverse management scenarios. These scenarios include emergency decision-making under sudden failures, reliability-cost trade-off analysis during design, and maintenance management. A case study of an urban rail train system validates the method, demonstrating its ability to accurately identify critical components whose failure results in a total loss of system reliability. Ultimately, the results confirm that this approach provides targeted decision support by effectively balancing computational efficiency and assessment accuracy across different operational departments.

Future research will expand this framework along two primary trajectories. First, system reliability assessment based on stochastic flow networks will be investigated under extreme environmental conditions, explicitly incorporating the cognitive uncertainty and heterogeneous behavioral responses of human personnel. Second, the integration of graph neural networks (GNNs) with reliability calculations represents a promising avenue to significantly accelerate computational efficiency, providing a scalable solution for the real-time analysis of large-scale CMSs.

Acknowledgment

This work is supported by the Shanghai Municipal Philosophy and Social Sciences Planning Youth Project (Grant: 2025EGL003).

References

1. Wang R, Xu J, Zhang W, Gao J, Li Y, Chen F. Reliability analysis of complex electromechanical systems: State of the art, challenges, and prospects. Quality and Reliability Engineering International 2022; 38(7): 3935–3969. https://doi.org/10.1002/qre.3175.
2. Singh P, Singh L K. State of knowledge correlation in failure analysis of mechatronics systems. IEEE Transactions on Reliability 2022; 72(1): 240–247. https://doi.org/10.1109/TR.2022.3172565.
3. Bouhali I, Pasquariello A, Mhenni F, Vitolo F, Hehenberger P, Patalano S, Choley J Y. Model-based systems engineering and safety assessment: A workflow for mechatronic systems design. Systems Engineering 2025; 28(2): 238 – 254. https://doi.org/10.1002/sys.21791.
4. Merschak S, Diallo T M, Hehenberger P. Life cycle sustainability assessment as a decision-making tool for the design of mechatronic systems. International Journal of Product Lifecycle Management 2022; 14(2-3): 142–173. https://doi.org/10.1504/IJPLM.2022.125823.
5. Jo J S, Kim S P, Oh S G, Kim T J, Kang F S, Park S J. Markov model-based reliability analysis considering the redundancy effect of modular converters. IEEE Access 2024; 12: 3328–3338. https://doi.org/10.1109/ACCESS.2023.3348832.
6. Jiang G J, Li Z Y, Qiao G, Chen H X, Li H B, Sun H H. Reliability analysis of dynamic fault tree based on binary decision diagrams for explosive vehicle. Mathematical Problems in Engineering 2021; 5559475. https://doi.org/10.1155/2021/5559475.
7. Akhtar I, Kirmani S. An application of fuzzy fault tree analysis for reliability evaluation of wind energy system. IETE Journal of Research 2022; 68(6): 4265–4278. https://doi.org/10.1080/03772063.2020.1791741.
8. Mehdi I, Boudi E M, Mehdi M A. Reliability, availability, and maintainability assessment of a mechatronic system based on timed colored Petri nets. Applied Sciences 2024; 14(11): 4852. https://doi.org/10.3390/app14114852.
9. Li Y F, Huang H Z, Mi J, Peng W, Han X. Reliability analysis of multi-state systems with common cause failures based on Bayesian network and fuzzy probability. Annals of Operations Research 2022; 311(1): 195–209. https://doi.org/10.1007/s10479-019-03247-6.
10. Yadav A D, Nandal N, Malik S, Malik S C. Markov approach for reliability-availability-maintainability analysis of a three unit repairable system. Opsearch 2023; 60(4): 1731–1756. https://doi.org/10.1007/s12597-023-00684-7.
11. Yi X J, Shi J, Cheng J. Reliability technology using GO methodology: A review. Quality and Reliability Engineering International 2019; 35(8): 2513–2539. https://doi.org/10.1002/qre.2541.
12. Liao W, Bak-Jensen B, Pillai J R, Wang Y, Wang Y. A review of graph neural networks and their applications in power systems. Journal of Modern Power Systems and Clean Energy 2021; 10(2): 345–360. https://doi.org/10.35833/MPCE.2021.000058.
13. Zhou T, Zhang X, Droguett E L, Mosleh A. A generic physics-informed neural network-based framework for reliability assessment of

multi-state systems. Reliability Engineering & System Safety 2023; 229: 108835. https://doi.org/10.1016/j.ress.2022.108835.

14. Huang C F, Huang D H, Lin Y K, Chen Y F. Network reliability evaluation of manufacturing systems by using a deep learning approach. Annals of Operations Research 2025; 348(1): 75–92. https://doi.org/10.1007/s10479-022-04911-0.
15. Huang T, Zhang Q, Tang X, Zhao S, Lu X. A novel fault diagnosis method based on CNN and LSTM and its application in fault diagnosis for complex systems. Artificial Intelligence Review 2022; 55(2): 1289–1315. https://doi.org/10.1007/s10462-021-09993-z.
16. Xiao N C, Yuan K, Zhan H. System reliability analysis based on dependent Kriging predictions and parallel learning strategy. Reliability Engineering & System Safety 2022; 218: 108083. https://doi.org/10.1016/j.ress.2021.108083.
17. Pan H, Yan J, Gao X, Fang J, Yao Z. Reliability assessment of integrated energy systems based on complex network theory. Engineering Reports 2023; 5(4): e12592. https://doi.org/10.1002/eng2.12592.
18. Gaur V, Yadav O P, Soni G, Rathore A P S. A literature review on network reliability analysis and its engineering applications. Proceedings of the Institution of Mechanical Engineers, Part O: Journal of Risk and Reliability 2021; 235(2): 167–181. https://doi.org/10.1177/1748006X20962258.
19. Lin S, Jia L, Zhang H, Wang Y. Reliability assessment of mechatronic systems considering multi covariates with system topology. Systems Engineering 2022; 25(1): 68–90. https://doi.org/10.1002/sys.21602.
20. Yin X, Mo Y, Dong C, Zhang Y. Identification of the influential parts in a complex mechanical product from a reliability perspective using complex network theory. Quality and Reliability Engineering International 2020; 36(2): 604–622. https://doi.org/10.1002/qre.2594.
21. He Z, Wang Y, Xia W, Shen Y, Hao Y, Ren Q. A method for reliability assessment of complex electromechanical system based on improved network connectivity entropy. Physica A: Statistical Mechanics and its Applications 2023; 632: 129331. https://doi.org/10.1016/j.physa.2023.129331.
22. Lin S, Wang Y, Jia L, Zhang H. Reliability assessment of complex electromechanical systems: A network perspective. Quality and Reliability Engineering International 2018; 34(5): 772–790. https://doi.org/10.1002/qre.2289.
23. Wang Z, Wang R X, Gao J M, Chen K, Liang Y J, Tang Z Z. Reliability prediction for GIL equipment based on multilayer directed and weighted network and failure propagation. IEEE Transactions on Reliability 2019; 69(4): 1207–1229. https://doi.org/10.1109/TR.2019.2923761.
24. Kubica J, Ahmed B, Muhammad A, Usama A M. Dynamic reliability calculation of random structures by conditional probability method. Eksploatacja i Niezawodność 2024; 26(2). https://doi.org/10.17531/ein/210685.
25. Liu X, An S. Failure propagation analysis of aircraft engine systems based on complex network. Procedia Engineering 2014; 80: 506–521. https://doi.org/10.1016/j.proeng.2014.09.108.
26. Xia W, Wang Y, Hao Y, He Z, Yan K, Zhao F. Reliability analysis for complex electromechanical multi-state systems utilizing universal generating function techniques. Reliability Engineering & System Safety 2024; 244: 109911. https://doi.org/10.1016/j.ress.2023.109911.
27. Liu J Q, Feng Y, Teng D, Jub-Yu C, Cheng L. Operational reliability evaluation and analysis framework of civil aircraft complex system based on intelligent extremum machine learning model. Reliability Engineering & System Safety 2023; 235: 109218. https://doi.org/10.1016/j.ress.2023.109218.
28. Tran H T, Domercant J C, Mavris D N. Parametric design of resilient complex networked systems. IEEE Systems Journal 2018; 13(2): 1496–1504. https://doi.org/10.1109/JSYST.2018.2825248.
29. Yeh C T, Lin Y K, Yeng L C L, Huang P T. Reliability evaluation of a multistate railway transportation network from the perspective of a travel agent. Reliability Engineering & System Safety 2021; 214: 107757. https://doi.org/10.1016/j.ress.2021.107757.
30. Bao M, Ding Y, Singh C, Shao C. A multi-state model for reliability assessment of integrated gas and power systems utilizing universal generating function techniques. IEEE Transactions on Smart Grid 2019; 10(6): 6271–6283. https://doi.org/10.1109/TSG.2019.2900796.
31. Lin K Y, Lin Y K. An algorithm for assessing a multistate resilience supply chain network in terms of system reliability. Annals of Operations Research 2025; 1–16. https://doi.org/10.1007/s10479-025-06769-4.
32. Yang X, He Y, Zhou D, Zheng X. Mission reliability–centered maintenance approach based on quality stochastic flow network for multistate manufacturing systems. Eksploatacja i Niezawodność 2022; 24(3): 455–467. https://doi.org/10.17531/ein.2022.3.7.
33. Chakraborty S, Goyal N K, Soh S. On area coverage reliability of mobile wireless sensor networks with multistate nodes. IEEE Sensors Journal 2020; 20(9): 4992–5003. https://doi.org/10.1109/JSEN.2020.2965592.

34. Huang D H. A generalized model to generate d-MP for a multi-state flow network. Computers & Industrial Engineering 2023; 179: 109205. https://doi.org/10.1016/j.cie.2023.109205.
35. Niu Y F, Wei J H, Xu X Z. Computing the reliability of a multistate flow network with flow loss effect. IEEE Transactions on Reliability 2023; 72(4): 1432–1441. https://doi.org/10.1109/TR.2023.3244955.
36. Chang P C, Huang D H, Huang C F. Simulation-based system reliability estimation of a multi-state flow network for all possible demand levels. Annals of Operations Research 2024; 340(1): 117–132. https://doi.org/10.1007/s10479-024-06141-y.
37. Lin Y K, Chen S G. An efficient searching method for minimal path vectors in multi-state networks. Annals of Operations Research 2022; 312(1): 333–344. https://doi.org/10.1007/s10479-019-03158-6.
38. Yeh W C. A novel node-based sequential implicit enumeration method for finding all d-MPs in a multistate flow network. Information Sciences 2015; 297: 283–292. https://doi.org/10.1016/j.ins.2014.11.007.
39. Mayag B, Bouyssou D. Necessary and possible interaction between criteria in a 2-additive Choquet integral model. European Journal of Operational Research 2020; 283(1): 308–320. https://doi.org/10.1016/j.ejor.2019.10.036.
40. Liu Y, Jiang W. A new distance measure of interval-valued intuitionistic fuzzy sets and its application in decision making. Soft Computing 2020; 24(9): 6987–7003. https://doi.org/10.1007/s00500-019-04332-5.
41. Lin S, Jia L, Zhang H, Zhang P, Xiong Y. Failure propagation analysis of high-speed train systems from the perspective of multi-layer stochastic flow network. Reliability Engineering & System Safety 2025; 111510. https://doi.org/10.1016/j.ress.2025.111510.
42. Zhang M, Yang N, Zhu X, Wang Y. A novel probabilistic linguistic multi-attribute decision-making method based on Mahalanobis–Taguchi system and fuzzy measure. Journal of the Operational Research Society 2024; 75(2): 246–261. https://doi.org/10.1080/01605682.2023.2188888.
43. Huang J J, Chen C Y. Leveraging the hierarchical symmetric 2-Additive Choquet Integral: Enhancing explainability and parallelizability in predictive models. Information Sciences 2024; 678: 121031. https://doi.org/10.1016/j.ins.2024.121031.
44. Fang R, Liao H. A 2-additive Choquet integral-based multi-criterion decision-making method with complex linguistic information in drug value assessment. Applied Soft Computing 2024; 152: 111198. https://doi.org/10.1016/j.asoc.2023.111198.
45. Laghridat C, Essalih M. A set of measures of centrality by level for social network analysis. Procedia computer science 2023; 219: 751–758. https://doi.org/10.1016/j.procs.2023.01.348.
46. Narukawa Y, Torra V. Scores for hesitant fuzzy sets: aggregation functions and generalized integrals. IEEE Transactions on Fuzzy Systems 2022; 31(7): 2425–2434. https://doi.org/10.1109/TFUZZ.2022.3226249.
47. Ashraf S, Ahmed M, Naeem M, Duodu Q. Novel Complex Intuitionistic Hesitant Fuzzy Distance Measures for Solving Decision‐Support Problems. Discrete Dynamics in Nature and Society 2024; 7498053. https://doi.org/10.1155/2024/7498053.
48. Mahmood T, Ali Z, Baupradist S, Chinram R. TOPSIS method based on Hamacher Choquet-integral aggregation operators for Atanassov-intuitionistic fuzzy sets and their applications in decision-making. Axioms 2022; 11(12): 715. https://doi.org/10.3390/axioms11120715.